CCA-1809

Resonance-Enhanced CARS Spectroscopy of Biliproteins

Siegfried Schneider, Franz Baumann, Ulrich Klüter*, and Peter Gege

Institut für Physikalische und Theoretische Chemie der Technischen Universität München, Lichtenbergstraße 4, D-8046 Garching, FR Germany

The theoretical and experimental aspects, which are involved in CARS spectroscopy of polyatomic molecules in liquid solution, are reviewed. Resonance-enhanced CARS spectra of various biliproteins (APC**, PC** and its subunits) from the cyanobacterium *Mastigocladus laminosus* in different states of aggregation are shown and discussed with respect to the information which can be derived about the structure of the tetrapyrrole chromophores. It is concluded that upon aggregation the chromophore properties are changed due to chromophore-protein interaction either by changes in conformation/configuration or by changes in the protein environment of the chromophores (microheterogeneity). Contrary to the widely accepted assumption, the chromophore geometry must be different in APC and PC.

INTRODUCTION

Information about molecular geometry can be derived from various spectroscopic techniques. X-ray spectroscopy, which provides, in a straightforward manner, information about bond lengths and bond angles, is preferentially applied to small molecules, where the sample is easily crystallized. For large molecules, like biological macromolecules, both the mathematical efforts to deduce the coordinates and the crystallization of the sample may give rise to complications[1].

Vibrational spectroscopic techniques like Raman spectroscopy, on the other hand, require less effort in sample preparation and give immediately structure specific information in the form of vibrational frequencies. Correlation between vibrational frequencies and molecular structure is, however, also complex. Computer programs, which solve the relevant eigenvalue problem, even for larger molecules, are being developed[2].

For the investigation of the chemical structure and/or geometry of chromophores of chromoproteins (a chromophore bound covalently to its so-called apoprotein)*** it is advisable to apply spectroscopic techniques, which use the

---

* New address: Agfa Gevaert, München.
** Abbreviations: Phycocyanin: PC, allophycocyanin: APC; phycobilisomes: PBS.
*** In the following, we will use the term chromophore »structure« to describe a certain chromophore-protein arrangement, that is a chromophore adopting a specific geometry and being subject to interactions with amino acid residues as e.g. proton transfer, hydrogen bonding or coulombic interaction.

effect of resonance enhancement. In the case of resonance Raman spectro-scopy, the wavelength of the incident radiation is resonant to an electronic transition of the chromophore. In the resonance Raman spectrum only vibra-tions of the chromophore are seen as the dominant bands. In contrast to other techniques like NMR or X-ray analysis, the signal of the chromophore is not covered up by the contribution of the protein with its more than 100-fold excess of atoms. For example, most of our knowledge on the photocycle of bacteriorhodopsin originates from resonance Raman spectroscopy[2].

The application of spontaneous resonance Raman spectroscopy is ham-pered, however, whenever the sample exhibits a strong fluorescence as in the case of biliproteins. Special experimental conditions like resonance with higher electronic states and/or low temperature were required for a successful attempt[3,4,5].

The important advantage of using coherent anti-Stokes Raman scattering (CARS) is that the wavelength of the scattered light, whose intensity has to be recorded, is shorter than that of the incident radiation. Therefore, no com-plications due to stray light and/or fluorescence occur.

During the last two years we have recorded a great number of CARS spectra of various biliproteins in various states of aggregation. In this contri-bution we want to give a review of our results and discuss their relevance with respect to molecular structure of the chromophores and the implications to the problem of energy transfer within the photosynthetic light harvesting systems of cyanobacteria and red algae, the so-called phycobilisomes. Since we believe that many readers are not familiar with either the technique or the peculiarities of the samples, we give a short introduction to both of these fields.

RESONANCE-ENHANCED COHERENT ANTI-STOKES RAMAN SPECTROSCOPY (CARS)

Theoretical Aspects and Line Shape Analysis

Coherent anti-Stokes Raman scattering (CARS) was first observed by Maker and Terhune[6]. With the advent of easily tunable dye lasers CARS spectroscopy became a very suitable tool for gaining vibrational spectra especially from fluorescing samples, which are not or only hardly accessible to investigations by spontaneous Raman spectroscopy (for reviews see e. g.[7,8,9]). In a typical CARS experiment two laser beams with frequencies ω_p (»pump«) and ω_s (»Stokes«) (with $\omega_p > \omega_s$) are focussed on the sample to produce a signal with frequency $\omega_c = \omega_p + (\omega_p - \omega_s)$ (see Figure 1a). From electrodynamics the inten-sity of that signal can be derived to be[10]:

$$I_c = \frac{256\,\pi^4}{c_o^4}\ \frac{\omega_c^2}{n_p^2\,n_s\,n_c}\ \left|\ \chi^{(3)}\ \right|^2\ I_p^2\,I_s\,l^2 \left(\frac{\sin\left(\dfrac{\Delta k \cdot l}{2}\right)}{\dfrac{\Delta k \cdot l}{2}}\right)^2 \tag{1}$$

with c_o : velocity of light in vacuum

   ω_c : $\omega_p + (\omega_p - \omega_s)$,

   $\omega_{c,p,s}$: CARS, pump, Stokes frequency, resp.

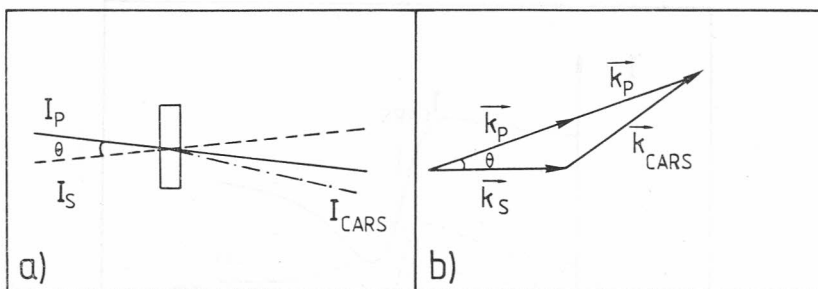$n_{c,p,s}$: index of refraction of the sample at frequency $\omega_{c,p,s}$, resp.

Figure 1. a) Generation of the CARS signal in the sample volume. b) The phase match condition.

$\chi^{(3)}$: third order susceptibility tensor of the sample, dependent on ω_p, ω_s

$I_{c,p,s}$: intensity of CARS, pump, Stokes beam, resp.

l : interaction length of pump and Stokes beam within the probed sample

$$\Delta k = |\, 2\vec{k}_p - \vec{k}_s - \vec{k}_c\,| \text{ with } |\vec{k}| = \frac{l}{\lambda} = \frac{n \cdot \omega}{2\pi\, c_o}$$

The last term in eq. 1 gives rise to the so-called phase match condition. Because of the frequency dependence of the index of refraction of the sample solution $(n = n(\omega))$, pump and Stokes beam must collide under a certain angle Θ to satisfy the phase match condition (eq. 2, see Figure 1b). It must be fulfilled for a macroscopic CARS signal to be generated.

$$\Delta k = |\, 2\vec{k}_p - \vec{k}_s - \vec{k}_c\,| = 0 \qquad (2)$$

Θ varies with both ω_p and ω_s; when scanning a CARS spectrum, a perfect phase match can be achieved only for one frequency difference $\omega_p - \omega_s$. In the actual experiment, a scan over approximately 500 cm^{-1} can be made with decreasing sensitivity towards both ends of the spectrum.

The third order susceptibility tensor $\chi^{(3)}$ is determined by the microscopic structural properties of the investigated molecules. If ω_p and/or ω_c are close to an allowed dipole transition of the molecule, the Raman bands strongly increase in intensity (resonance-enhanced CARS)[10,11,12]. In this case and dealing with one molecular vibration r only, $\chi^{(3)}$ can be approximated by[8,13]:

$$\chi^{(3)} = B + \frac{R_r + iI_r}{\delta_r - i\Gamma_r} \qquad (3)$$

with B : nonresonant background term (mostly assumed to be constant and real over the region of a CARS spectrum)

R_r, I_r : real and imaginary part of the resonance enhanced term due to the chromophore(s)

Γ_r : Raman line-width

$\delta_r = \nu_r - (\nu_p - \nu_s)$ with ν_r = wavenumber of molecular vibration r, ν_p, ν_s wavenumber of pump and Stokes beam, resp.
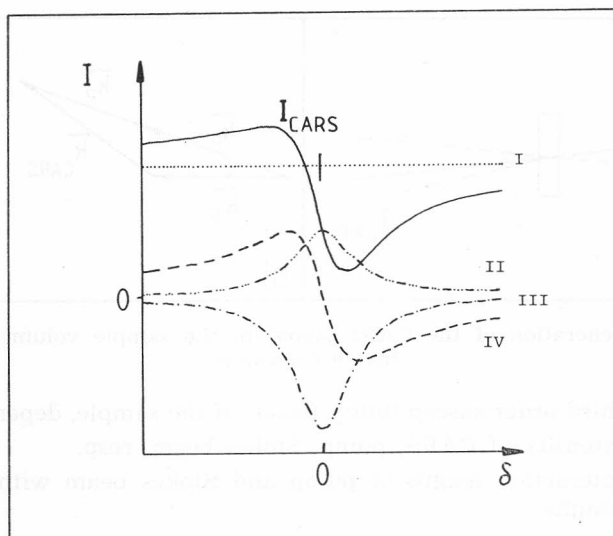
Figure 2. Contributions to the CARS intensity according to eq. 4.

In this approximation the CARS intensity I_c (see also Figure 2), due to molecular vibration r can be written as

$$I_c(\delta) \sim |\chi^{(3)}|^2 = B^2 + \frac{R_r^2 + I_r^2}{\delta_r^2 + \Gamma_r^2} - \frac{2BI_r\Gamma_r}{\delta_r^2 + \Gamma_r^2} + \frac{2B\delta_r R_r}{\delta_r^2 + \Gamma_r^2} \tag{4}$$

$$\text{I} \qquad\qquad \text{II} \qquad\qquad \text{III} \qquad\qquad \text{IV}$$

It is theoretically and experimentally well established that the shape of a CARS line depends on the difference between the frequencies of the pump laser and the electronic transition (absorption maximum)[8,13,14]. It is convenient to classify the various forms as positive Lorentzian (Figure 3a), right dispersive (Figure 3b), negative Lorentzian (Figure 3c) and left dispersive (Figure 3d), depending on the relative size of B, $R_r(\omega_p)$ and $I_r(\omega_p)$. For the realistic case of more than one normal mode, eq. 4 is replaced by:

$$|\chi^{(3)}|^2 = \left| B + \sum_{r=1}^{n} \frac{R_r + iI_r}{\delta_r - i\Gamma_r} \right|^2 =$$

$$= \left\{ B + \sum_{r=1}^{n} \frac{R_r\delta_r - I_r\Gamma_r}{\delta_r^2 + \Gamma_r^2} \right\}^2 + \left\{ \sum_{r=1}^{n} \frac{I_r\delta_r + R_r\Gamma_r}{\delta_r^2 + \Gamma_r^2} \right\}^2 \tag{5}$$

B : nonresonant background.

R_r, I_r : real and imaginary part of the resonance-enhanced term of the molecular vibration ν_r.

Γ_r : Raman line-width of vibration ν_r.

δ_r : $\nu_r - (\nu_p - \nu_s)$ with ν_r, ν_p, ν_s wavenumber of molecular vibration, pump and Stokes laser, resp.

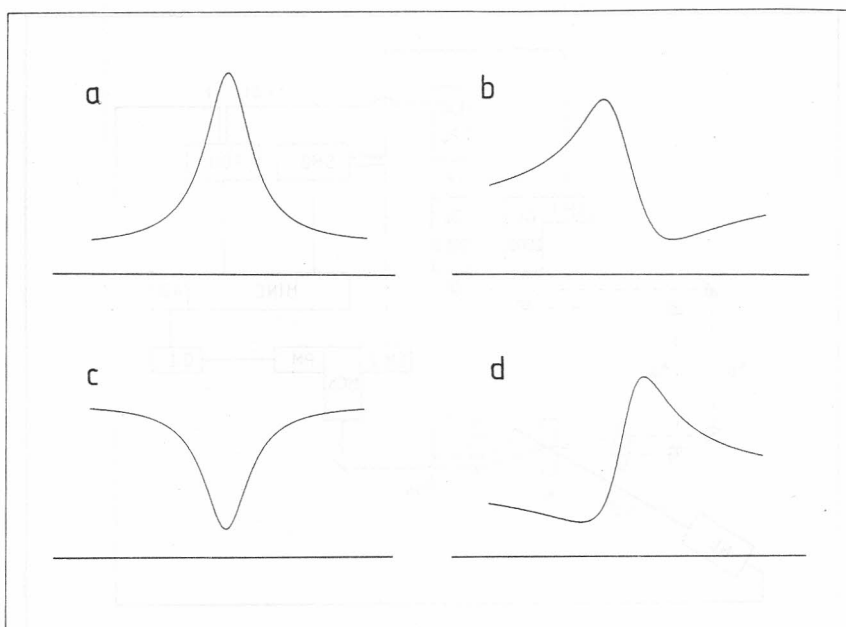n : number of vibrations which contribute to $\chi^{(3)}$.

Figure 3. Classification of CARS line-shapes: a) positive Lorentzian, b) right dispersive, c) negative Lorentzian, d) left dispersive.

Especially in the case of several close-lying vibrational frequencies ν_r, the evaluation of CARS spectra can be complicated by the interference of bands with dispersive line-shapes. However, these problems can be overcome by either using the appropriate pump frequency to produce spectra with positive Lorentzian bands (like in spontaneous Raman spectroscopy), or by making a line-fit of the spectrum. Besides, a comparison of CARS spectra recorded with different pump frequencies can provide additional information and thus help evaluate complicated vibrational spectra.

When starting our line-fit procedure, the parameters describing each of the bands in a certain vibrational region are determined separately by single line-fits of small sections of the experimental spectrum (see eq. 4). Then, these single line-fits are combined and parameters B, R_r, I_r, ν_r, Γ_r are varied to fit the function (eq. 5) to the CARS spectrum with least mean squares. To establish a suitable set of starting parameters for the fitting procedure and to test whether a fit is unequivocal, it has proved to be highly advantageous to use also a line-modelling program, which calculates and draws a spectrum according to differently chosen parameters.

The fitting is performed on a personal computer (IBM XT286) using the simplex algorithm[14,15,16]. It has the advantage to fit functions to data without using derivatives or numerical differentiations and no matrix operation is involved. Therefore, it is possible to fit many parameters (e. g. 17 for 4 vibrations) to data (e. g. one CARS spectrum consists of 500 data points) within an acceptable time even on a personal computer.
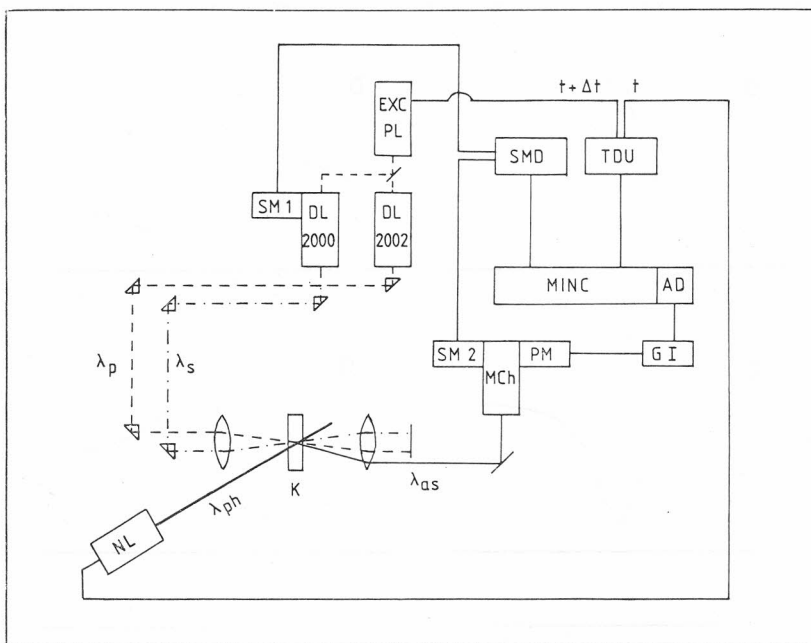
Figure 4. Experimental arrangement for recording resonance-enhanced CARS spectra: NL = nitrogen laser, DL = dye laser, EXC PL = excimer pump laser, SM = stepping motor, SMD = stepping motor driving unit, TDU = trigger delay unit, MINC = computer, AD = analog digital converter, GI = gated integrator, MCh = monochromator, PM = photomultiplier.

ANTENNA PIGMENTS

A major problem for photosynthetic organisms is the adaptation to varying light conditions. To this end cyanobacteria, red algae and cryptophytes have developed biliproteins (open chain tetrapyrrole chromophores bound to the apoprotein via a thioether bridge, see Figure 5) as light harvesting antenna pigments (for recent reviews see *e. g.*[19-22]). These pigments enlarge the spectral (Figure 6) and geometrical cross section for the absorption of light. In cyanobacteria and red algae, biliproteins with different absorption maximum are assembled in the so-called phycobilisomes. They are built of rods containing phycocyanin (PC) and phycoerythrocyanin (PEC) (or phycoerythrin in some organisms), attached in a semicircular way to allophycocyanin (APC) (see Figure 7)[23-25]. The spatial arrangement of the biliproteins guarantees a highly efficient transfer of the excitation energy along the transfer chain PEC — > PC — > APC to the chlorophylls in the photosynthetic membrane, where the excitation energy is at last converted into chemical energy as ATP and NADPH.

Picosecond time-resolved spectroscopy (fluorescence and ground state recovery) revealed many aspects of the excitation transfer kinetics and proved the sensitivity of the energy transfer times on several parameters like state of aggregation or denaturation, or the presence of so-called linker polypeptides. The latter are important for the arrangement of the hexameric units in
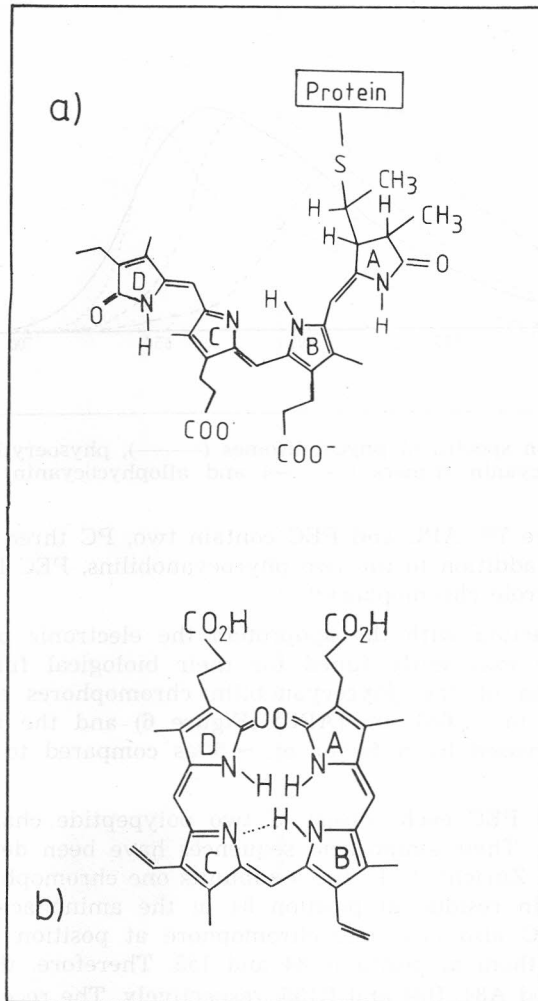
Figure 5. Chemical structure of chromophores: a) phycocyanobilin with extended geometry (PC), b) biliverdin IX, in biliprotein of *Pieris brassicae*.

the phycobilisomes, but do not contain chromophores (see e. g.[26-33]). A quantitative understanding of the energy transfer processes was, however, not possible before the amino acid sequences and details of the three-dimensional structure were determined.

At present, the phycobilisomes of the cyanobacterium *Mastigocladus laminosus* and especially its phycocyanin are among the best characterized biliproteins. Some results of the various investigations, which have been performed to enlighten their organization and function, are shortly summarized in the following.

The phycobilisomes of *Mastigocladus laminosus* consist of APC, PC and PEC, forming trimeric or hexameric discs, which are assembled in the PBS,
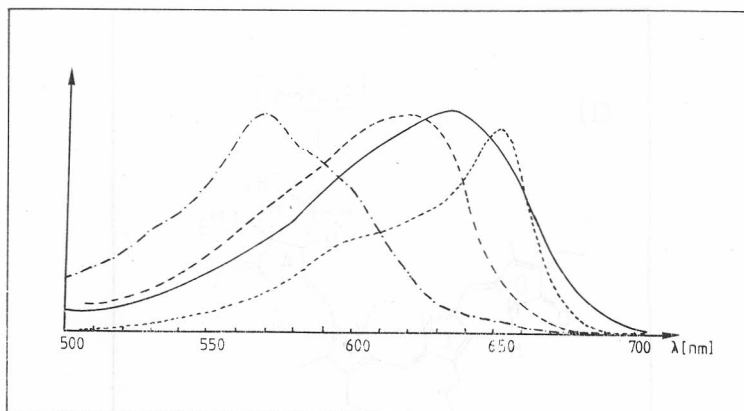
Figure 6. Absorption spectra of phycobilisomes (———), physoerythrocyanin trimers (— · — · —), phycocyanin trimers (— — —) and allophycocyanin trimers (- - - - -).

as shown in Figure 7[25]. APC and PEC contain two, PC three phycocyanobilin chromophores; in addition to the two phycocyanobilins, PEC has another, still unknown tetrapyrrole chromophore[34].

By the interaction with the apoprotein the electronic properties of the chromophores are excellently tuned for their biological function. *E. g.* the absorption maxima of the phycocyanobilin chromophores are varied from ≈ 570 nm (PEC) to ≈ 650 nm (APC) (Figure 6) and the long wavelength absorption is increased by a factor of ~ 5 as compared to a free chromophore[22,34].

APC, PC and PEC each consist of two polypeptide chains, the socalled α- and β-subunits. Their amino acid sequences have been determined by the group of Zuber in Zürich[34-37]. In the α-subunits one chromophore is covalently bound to a cystein residue at position 84 in the amino acid sequence. The β-subunits of APC also bear one chromophore at position 84, those of PC and PEC two of them at positions 84 and 155. Therefore, the chromophores are usually denoted A84, B84 and B155, respectively. The recent determination of the three-dimensional structure of PC trimer crystals by X-ray analysis provided an enormous help for the understanding of spectral and kinetic properties of the chromophores and their interaction with the apoprotein[1,38] It was revealed that in PC trimers the chromophores A84 and B84 are located close-by, embedded in a similar protein environment, and exhibit a similar (extended) geometry (Z-anti, Z-syn, Z-anti at the methine bridges between ring A—B, B—C and C—D, resp.). Chromophore B155 is quite different both in environment and chromophore geometry (Z-anti, Z-syn, Z- or E-anti).

A prerequesite for promising investigations concerning the structure and function of biliproteins is the availability of welldefined samples. During the last ten years biochemists have succeeded in developing procedures which yield reliable and reproducible preparations of phycobilisomes, their subunits and suitable model compounds.
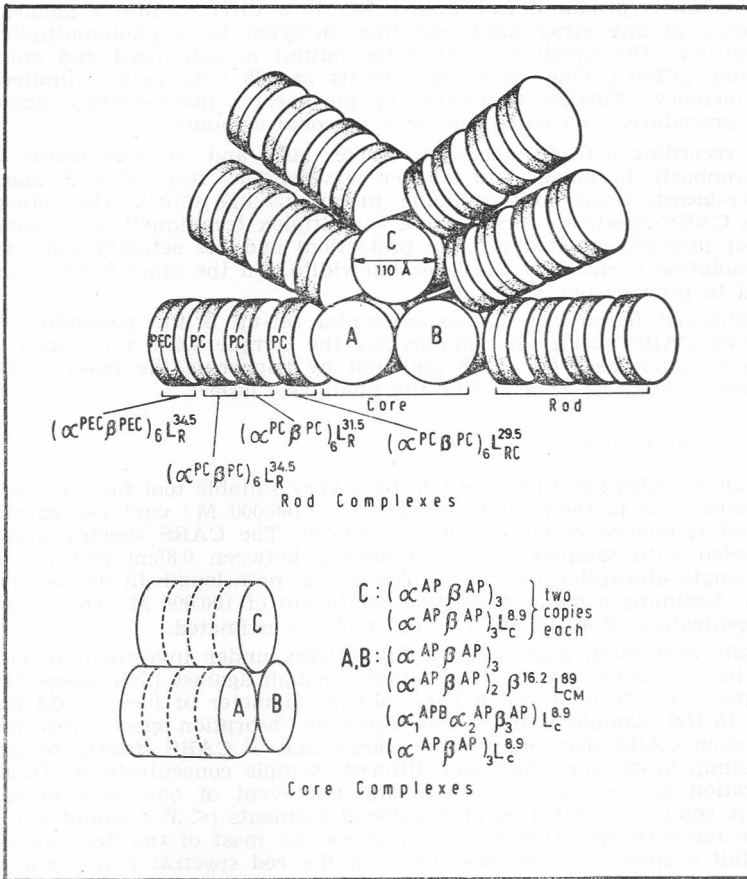
Figure 7. Phycobilisome models of *Mastigocladus laminosus*. The core is built up of allophycocyanin (here denoted as AP), the periphery of phycocyanin (PC) and phycoerythrocyanin (PEC). In each part various linker polypeptides (L) are contained. (Adapted from Ref. [25]).

MATERIALS AND METHODS

a) Sample Preparation

The samples which we used during the work described in this contribution were provided by Prof. Scheer and his group. We very much appreciate their cooperation.

The investigated samples, prepared according to well-established procedures, were dissolved in different aqueous potassium phosphate buffers (KPB): PBS (900 mM KPB, pH 6)[39], PC (100 mM KPB, pH 7),[40] β-subunits of PC (20 mM KPB, pH 7)[40] and APC (5 mM KPB, pH 7.1)[41]. All these preparations originate from the cyanobacterium *Mastigocladus laminosus*.

b) The CARS Apparatus

A schematic of the CARS apparatus is given in Figure 4[14]. Two dye lasers, both pumped by one excimer laser, produce the pump and Stokes beam, resp. These are focussed into the sample cuvette under the phase match angle. There,

the CARS beam is produced (see Figure 1a). It is directed into a monochromator for separation of any stray light and then detected by a photomultiplier and a gated integrator. The integrator's analogue output is digitalized and stored by a minicomputer (MINC). One spectrum consists of 500 data points (limited by the computer memory). Further evaluation of the spectra (peak-finding, smooth, plot or line-fit procedures) is carried out on a personal computer.

When recording a CARS spectrum, Stokes laser and monochromator are scanned synchronously to longer and shorter wavelengths, resp. This is managed by a computer-based, home-built stepping motor driving unit[14]. The advantage of scanning a CARS spectrum versus using a multiplex technique[17] is the much lower Stokes laser intensity applied (sample protection) and the actually achieved higher spectral resolution (limited by the laser linewidth). On the other hand, many pulses are needed to produce one spectrum.

An additional feature of our experimental set-up is the possibility to record time-resolved CARS spectra by photolyzing the sample with a nitrogen ($\lambda_{ph} = 337$ nm) or an excimer laser ($\lambda_{ph} = 308$ nm) and by triggering the pump/Stokes lasers with a present delay (≥ 25 ns) after the photolysis laser[18].

c) *Experimental Parameters*

Resonance CARS has turned out to be a very suitable tool for the investigation of biliproteins. Due to their high absorption ($\approx 100{,}000$ M^{-1} cm^{-1} per chromophore), a very good resonance enhancement is achieved. The CARS spectra shown below were recorded with samples of optical density between 0.8/cm and 1.5/cm at the long wavelength absorption maximum. The optical path length in the sample cuvette was 2 mm. Assuming a molar extinction coefficient of 100,000 M^{-1} cm^{-1} [42], a chromophore concentration of $4 \cdot 10^{-5}$ to $7.5 \cdot 10^{-5}$ mol/l is estimated.

As light harvesting pigments, all biliproteins under investigation, even when separated into subunits, proved to be stable enough against high power laser irradition (typical: $\tau \approx 20$ ns, $I_p \approx 1$ mJ, $I_s \approx 0.5$ mJ, diameter of focus ≈ 0.4 mm, repetition rate 10 Hz). Sample stability was tested by absorption spectra recorded before and after each CARS scan and by the comparison of CARS spectra recorded with different pump beam intensities and different sample concentrations. Thus, a relevant alteration of the sample, also during the event of one laser pulse, can be excluded. A small concentration of denatured pigments ($< 5\%$) would not however, change the recorded spectrum for two reasons: (a) most of the decomposition products exhibit a smaller, or no absorption in the red spectral region and (b) there is a relative high threshold for the generation of the (non-linear) CARS signal.

d) *Dispersive Line-shape*

A feature which is often believed to limit the versatility of CARS spectroscopy is the occurrence of dispersive line-shapes, which may complicate of affect a reliable evalution of CARS spectra. However, this problem can often be fairly easily overcome by selecting a suitable pump wavelength, for which spectra with positive Lorentzian bands are produced. These can be evaluated as easily as spontaneous (resonance) Raman spectra.

Examples of the effect of a change of pump wavelength are given in Figure 8 (trace a and b). It displays the spectra recorded for trimers of PC with pump wavelength $\lambda_p = 584$ nm (trace a) and 640 nm (trace b), respectively. A bathochromic shift of the pump wavelength changes the appearance of the vibrational bands from right dispersive to positive Lorentzian (notation see Figure 3). Even in a spectrum with a dispersive line-shape, like the one shown in Figure 8a, the essential features can be determined without great effort. Strong bands are found at 1052, 1112, 1364/77, 1580/97 and 1647/67 cm^{-1}; several partially overlapping bands appear in the fingerprint region between 1200 and 1300 cm^{-1}. For highly dispersive bands, the frequency of the molecular vibrations cannot be determined exactly without a detailed analysis (linefit program). In the case of well separated bands, at least a small interval can be easily determined (*e. g.* 1364/77 cm^{-1}) as the exact wavenumber of the vibration must range between those of maximum and minimum intensity[13].
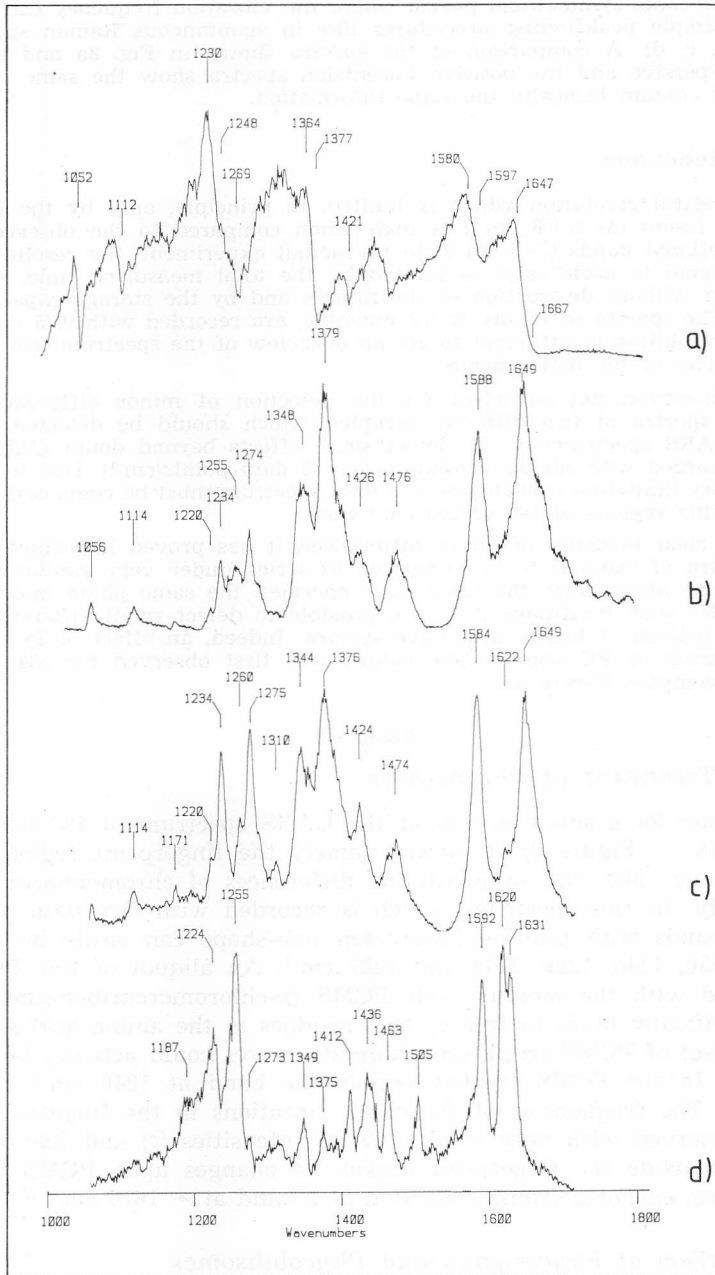
Figure 8. Resonance CARS spectra of: a) phycocyanin trimers ($\lambda_p = 584$ nm), b) phycocyanin trimers ($\lambda_p = 640$ nm), c) phycobilisomes ($\lambda_p = 640$ nm), d) biliprotein from *Pieris brassicae* ($\lambda_p = 640$ nm).

Nevertheless, it is easier to evaluate spectra with positive Lorentzian line-shapes (small background, symmetrical peaks) where the vibration frequency can be determined by simple peakfinding procedures like in spontaneous Raman spectroscopy (Figures 8b, c, d). A comparison of the spectra shown in Fig. 8a and 8b reveals that the dispersive and the positive Lorentzian spectra show the same vibrational pattern and contain basically the same information.

e) CARS Resolution

The spectral resolution which is limited, in principle, only by the line-width of the two lasers ($\Delta \nu \leq 0.6$ cm^{-1}) is high when compared to the observed widths of the vibrational bands (> 5 cm^{-1}). In the actual experiment, the resolution, given a certain signal to noise ratio, is limited by the total measuring time, which can be employed without destruction of the sample and by the storage capacity of the computer. The spectra of Figure 8, for example, are recorded with 0.75 data points/ /cm^{-1}. The resolution is sufficient to get an overview of the spectrum and to deduce the frequencies of the major bands.

It is, however, not sufficient for the detection of minor differences in the vibrational spectra of two different samples, which should be detected by application of CARS spectroscopy. To detect small effects beyond doubt CARS spectra must be recorded with higher resolution (2 ... 5 data points/cm^{-1}). Due to our computer memory limitation (500 channels) a total spectrum must be composed of several scans, covering regions of 100 or 200 cm^{-1} each.

To get clear evidence of minor differences, it has proved important to record CARS spectra of samples to be compared in series under very similar conditions (*e. g.* the same absorbance, the same laser energies, the same phase matching condition). Under such conditions it is also possible to detect small differences in the vibrational pattern of highly dispersive spectra. Indeed, an effect of PCMS on the CARS spectrum of PC trimers (see below) was first observed for 584 nm pump frequency (compare Figure 8a).

RESULTS

a) PCMS-Treatment of Phycocyanin

In Figure 9a a small section of the CARS spectrum of PC trimers (the same sample as Figure 8) is shown, namely the fingerprint region between 1200 cm^{-1} and 1300 cm^{-1} in which the differences of chromophores show up most clearly. In this spectrum, which is recorded with five data points per cm^{-1}, six bands with positive Lorentzian line-shape can easily be identified at 1220, 1236, 1246, 1259, 1274 and 1287 cm^{-1}. An aliquot of this PC sample was treated with the mercury salt PCMS (*p*-chloromercuribenzenesulfonate) which specifically binds to free cystein residues in the amino acid sequence[42].

An effect of PCMS on chromophore structures could actually be revealed by CARS. In the PCMS treated sample the band at 1246 cm^{-1} disappears (Figure 9). The frequencies of the other vibrations in the fingerprint region are all preserved with very similar CARS intensities (ρ) and line-widths (Γ) (Table I). Outside the fingerprint region, no changes upon PCMS treatment are observed, except a strong reduction of a band at ~ 1670 cm^{-1} [43].

b) Comparison of Phycocyanin and Phycobilisomes

Highly resolved resonance CARS spectra of PBS ($\lambda_p = 640$ nm), PC trimers ($\lambda_p = 640$ nm) and APC trimers ($\lambda_p = 640$ nm and 655 nm), the latter two without linker peptides, are shown for comparison in Figures 10a, b and 12, ab, respectively. The PBS spectra are very similar to the PC trimer spectra,
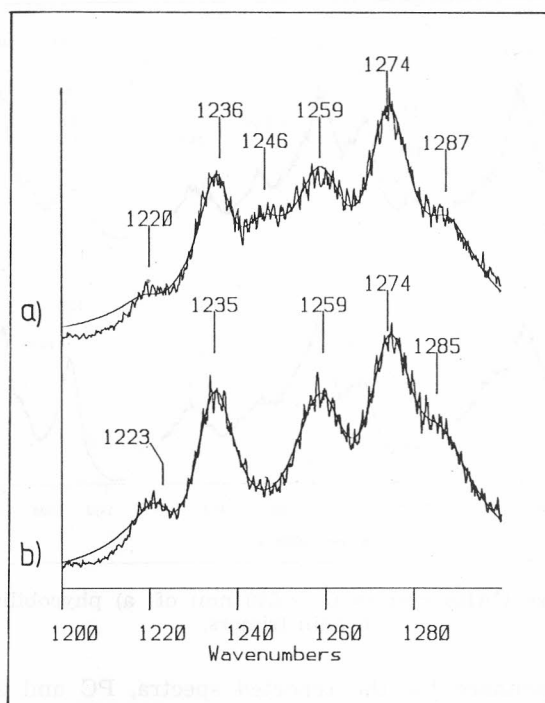
Figure 9. Resonance CARS spectra of PC trimers ($\lambda_p = 640$ nm) in the fingerprint region: a) untreated sample, b) sample fully titrated with PCMS. The solid lines represent the resulting fit-functions according to the parameters listed in Table I.

TABLE I

Resulting Fit Parameters for the CARS Spectra of PC Trimers Untreated (top) and Titrated (Bottom) with PCMS. The Spectra are Displayed in Figure 9 ($\lambda_p = 640$ nm). ν: Frequency of Vibration (cm^{-1}), Γ: Line-width (cm^{-1}), $\varrho = (R^2 + I^2)^{1/2}$: CARS Intensity, $\alpha = Arctan(R/I)$, (See Equations 3, 5)

ν	1220.1	1236.0	1246.2	1259.1	1274.0	1287.1
Γ	5.1	4.7	8.0	8.1	6.4	7.0
ϱ	0.7	3.7	2.8	4.6	5.7	2.4
α	282	270	269	271	272	271
ν	1223.2	1234.8	—	1259.5	1274.1	1285.2
Γ	5.8	6.3	—	8.1	6.9	7.7
ϱ	2.6	6.4	—	5.6	6.9	3.0
α	282	232	—	274	266	259

supposedly due to the dominance of PC in PBS of *Mastigocladus laminosus*[25]. The presence of APC shows up in the weak peak at 1623 cm⁻¹.

Very important information can be gained from the comparison of the apparent linewidth of PC and PBS bands in the double bond stretching region (1500—1750 cm⁻¹). Though PBS are built up of several building stones (PE,
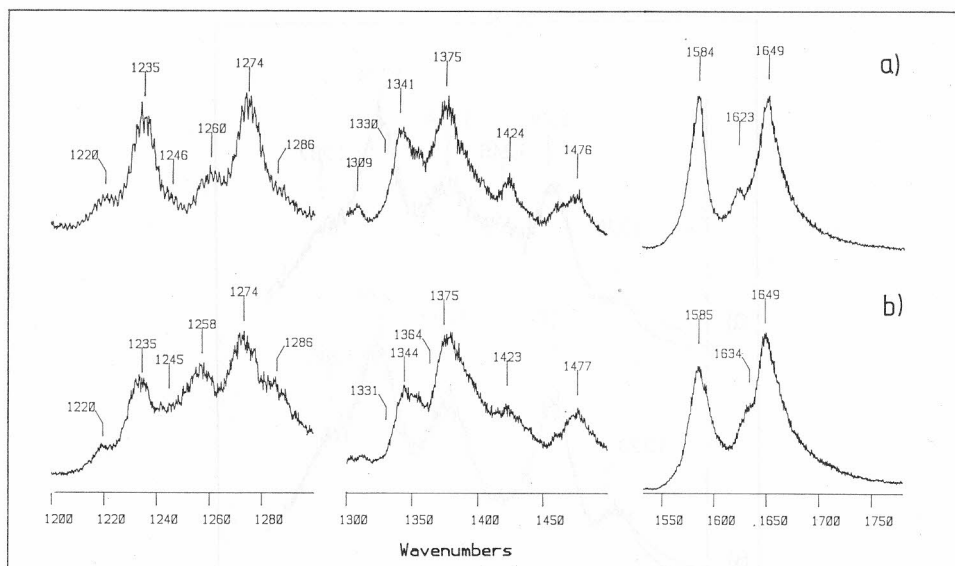
Figure 10. Resonance CARS spectra (λ_p = 640 nm) of: a) phycobilisomes, b) phyco-
cyanin trimers.

which was off resonance for the reported spectra, PC and APC, each with
different linker peptides) the apparent width of the 1584 cm^{-1} ($\Gamma = 18.0$ cm^{-1})
and 1649 cm^{-1} ($\Gamma = 26.3$ cm^{-1}) peaks are distinctly smaller than in PC trimers
without linker peptides (1585 cm^{-1} : $\Gamma = 26.3$ cm^{-1}; 1649 cm^{-1} : $\Gamma = 30.5$).

c) *β-Subunits*

Figure 11 presents resonance CARS spectra of PC trimers from *Mastigo-
cladus lamniosus* and their β-subunits. In the used buffer solution (20 mM
potassium phosphate buffer, pH 7) the β-subunits form preferentially dimers[44].
Again, the fingerprint region between 1200 cm^{-1} and 1300 cm^{-1} and the double
bond stretching region (1500—1750 cm^{-1}) show strong differences. In the latter,
the two prominent bands at ~ 1590 cm^{-1} and ~ 1650 cm^{-1} are significantly
broader in the β-subunit spectrum and the maxima of the (positive Lorentzian)
peaks are shifted (PC-trimer: 1588/1648 cm^{-1}, β-subunit: 1594/1654 cm^{-1}). In
the fingerprint region several peaks found for PC trimers are lacking in the
β-subunit spectrum (1221 cm^{-1}, 1236 cm^{-1}).

Contrary to our expectation, we did not observe any influence of PCMS
titration on the CARS spectra of the β-subunit. This is surprising since the
only reactive free cystein is located at the β-subunit (B111).

It should be noted that the CARS spectra of PC trimers displayed in
Figure 10b and Figure 11b, respectively, were recorded on different days
and originate from different preparations. Their identity proves that both
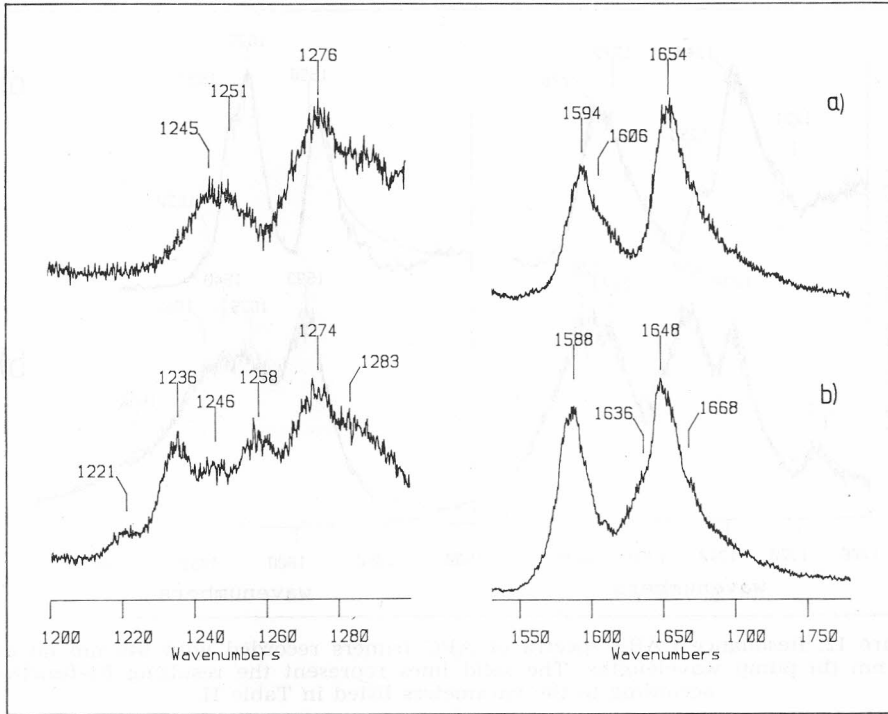preparation and CARS measurement are excellently reproducible.

Figure 11. Resonance CARS spectra ($\lambda_p = 640$ nm) of: a) β-subunits of PC, b) PC trimers.

d) Allophycocyanin

Figures 12a and 12b compare highly resolved CARS spectra of APC trimers without linker peptides, $(\alpha^{APC} \beta^{APC})_3$, recorded with different pump wavelengths: 640 nm and 655 nm, resp. While the 655 nm spectrum appears positive Lorentzian, the 640 nm spectrum is slightly right dispersive. Therefore, an exact comparison of the vibrations is facilitated by the application of the line-fit procedure (see above)[14,16]. In the central parts of the spectra a very good agreement of the fit-functions with the recorded spectra is achieved. The poorer quality of the fits at the edges of the recorded spectra is due to the interference of bands lying just outside the recorded part of the spectrum. In the double bond stretching region the spectrum recorded for $\lambda_p = 640$ nm could be fitted by using the parameters given in Table II. Because of the relative poor signal to noise ratio and the very broad width of the band in the spectrum recorded for $\lambda_p = 655$ nm, an unequivocal fit of the spectrum is not possible. Therefore, we first modelled that spectrum using the fixed parameters ν and Γ taken from the fit of the APC spectrum recorded for $\lambda_p = 640$ nm. Then we started the fit procedure. In Table II the resulting fit parameters are listed for comparison. In the fingerprint region the spectra are well approximated by a fit with five vibrations. Their frequencies (ν) and linewidths (Γ) correspond quite nicely, whereas their relative intensities $\rho = (R^2 + I^2)^{1/2}$ differ (Table II).
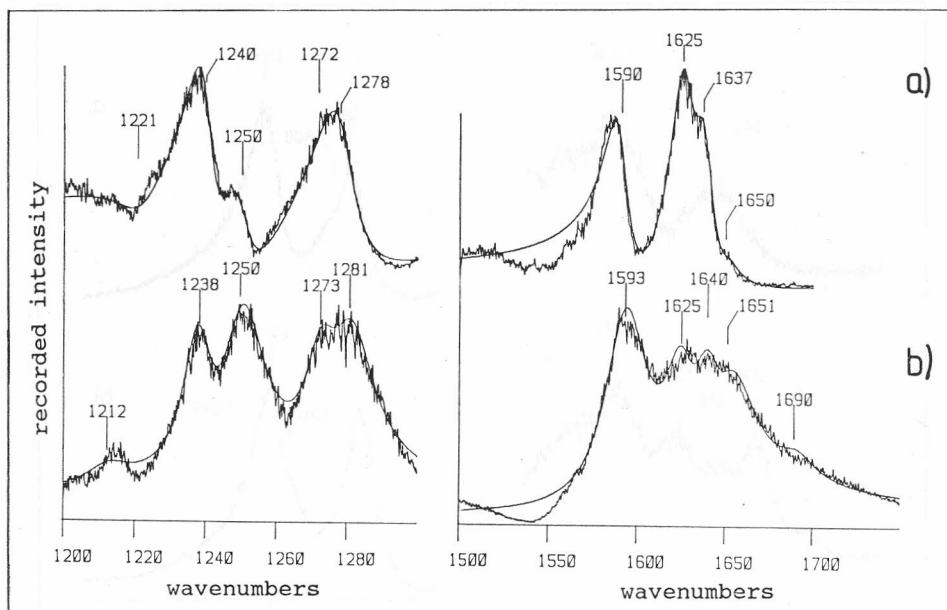
Figure 12. Resonance CARS spectra of APC trimers recorded with 640 nm (a) and 655 nm (b) pump wavelengths. The solid lines represent the resulting fit-functions according to the parameters listed in Table II.

TABLE II

Resulting Fit Parameters for the CARS Spectra of APC, Displayed in Figure 12, Recorded with λ_p = 640 nm and 655 nm, resp. ν: Frequency of Vibration (cm^{-1}), Γ: line-width (cm^{-1}), ϱ = (R^2 + I^2)$^{1/2}$: CARS Intensity, α = Arctan(R/I), (See Equations 3, 5)

λ_p	640 nm	655 nm	640 nm	655 nm
ν	1221.6	1212.3	1590.4	1593.4
Γ	9.2	7.3	8.4	14.3
α	94	234	335	233
ϱ	1.07	0.50	5.80	5.39
ν	1240.3	1238.1	1625.6	1625.4
Γ	4.2	4.8	8.5	10.3
α	0	257	316	274
ϱ	3.47	2.15	6.56	2.89
ν	1250.1	1250.2	1637.5	1640.4
Γ	5.0	7.2	7.1	10.2
α	0	248	328	271
ϱ	2.41	2.68	4.87	3.38
ν	1272.0	1272.6	1650.1	1651.3
Γ	8.0	5.5	5.5	13.2
α	331	276	264	218
ϱ	0.75	1.46	0.95	3.29
ν	1277.9	1281.2	—	(1690.4)
Γ	6.5	7.5	—	(12.2)
α	329	273	—	(274)
ϱ	3.59	2.16	—	(0.75)

e) The Pieris brassicae Pigment

In Figure 8d an overview resonance CARS spectrum of a biliprotein is shown, which is distinctly different from the phycobiliproteins presented above. It originates from the butterfly *Pieris brassicae*. Although the pigment's biological function is still under debate,[45] spectral properties of the chromophore and a three-dimensional structure of the crystallized protein have been determined recently[46,47]. The chromophore (biliverdin IX$_\gamma$, see Figure 5b) is not covalently bound to the apoprotein. In contrast to the phycocyanobilin chromophore of PC, it is embedded in a cyclic helical geometry in the apoprotein[46,47].

The resonance CARS spectrum (Figure 8d) shows some characteristic features. In the fingerprint region only two prominent (right dispersive) bands arise at 1224/1234 cm^{-1} and 1255/1270 cm^{-1} and a weak one at 1276/1281 cm^{-1}. Between 1300 cm^{-1} and 1520 cm^{-1} a series of well-resolved bands with rather positive Lorentzian line-shape shows up at 1349, 1375, 1412, 1436, 1463 and 1505 cm^{-1}. In the double bond stretching region three very intensive (positive Lorentzian) bands appear at 1592 cm^{-1} and at 1620 cm^{-1} and 1631 cm^{-1} (shoulder). The apparent linewidths are comparatively small: 14 cm^{-1} for the band at 1595 cm^{-1} and 20 cm^{-1} for the double band 1620/1635 cm^{-1}.

DISCUSSION

Up till now, trimeric PC from the cyanobacterium *Mastigocladus laminosus* is the biliprotein which has been investigated most intensively by CARS spectroscopy. As this pigment is also well studied by many other methods (see sect. Antenna Pigments), it is a good starting point for the characterization of biliproteins by vibrational spectra and an assignment of observed bands. Especially the determination of the three-dimensional protein structure and the extended chromophore geometries by X-ray analysis is a very valuable aid.

Two spectral ranges have experimentally proved to be best suited for the examination of PBS, PC and APC samples by CARS spectroscopy. The first one is the fingerprint region between 1200 cm^{-1} and 1300 cm^{-1} with a number of well resolved bands, which are a highly sensitive probe for the geometry and environment of the chromophores. The second range is the double bond stretching region between 1550 cm^{-1} and 1750 cm^{-1}. There the dominant vibrations should mainly originate from the pyrrole rings ($\sim$ 1590 cm^{-1}) and the methine bridges connecting them. This is judged from normal mode calculations, which predict rather localized C=C vibrations (ν: 1590 cm^{-1} -- 1670 cm^{-1}) at the methine bridges[48,49,50] and the inspection of CARS spectra of different biliproteins with different conformation/configuration (see below).

a) PCMS Treatment of Phycocyanin

An example of the significance of these vibrational regions is the PCMS treatment of PC trimers (see Figure 9). The disappearance of the 1246 cm^{-1} and $\sim$ 1670 cm^{-1} vibrations, whereas the rest of the spectrum is perfectly preserved, can be rationalized (provided that these vibrations are rather localized) by assuming that only a part of one phycocyanobilin chromophore is affected by PCMS. The structural change probably occurs in the ring C-ring D fragment (see Figure 5a) of chromophore B84, which is located closest to the in-

serted salt (X-ray analysis[38,51]). The two affected bands might originate from the methine bridge between rings C and D (1670 cm^{-1} : C=C stretching vibration, 1246 cm^{-1} : C—H in plane bending/C—C stretching vibration).

Another possible explanation could be a change in the »microheterogeneity« of the B84-chromophores, which means a variation of the accessible structures (chromophore-protein arrangement) by the presence of another big molecule in the neighbourhood of the chromophore. A detailed discussion of this problem, including results of picosecond time-resolved fluorescence measurements can be found in references[52,53].

b) Comparison of Phycocyanin and Phycobilisomes

The dependence of the microheterogeneity on the state of aggregation is illustrated by a comparison of PC trimer (without linker peptides) and PBS spectra (Figure 10). The PBS spectrum is, due to the excess of PC in PBS (Figure 7) dominated by the contribution of PC. Nevertheless, the prominent bands around 1584 cm^{-1} (pyrrole rings) and 1649 cm^{-1}, probably originating from methine bridge C=C-vibrations, show a significantly smaller linewidth for PBS than for PC trimers without linker peptides. The presence of linkers seems to favour the formation of certain better defined structures. Recently recorded CARS spectra of PC hexamers containing a linker peptide (samples kindly provided to us by Dr. R. Rümbeli) support this conclusion.

c) Comparison of β-subunits and Phycocyanin

Another example of the effect of aggregation and/or preparation on chromophore structure is provided by CARS spectra of β-subunits of PC, which contain two (B84, B155) of the three PC chromophores (see section Antenna Pigments). Again, a significant broadening of the prominent bands in the double bond stretching region can be observed, though the number of different kinds of chromophores is reduced from 3 to 2. Besides, the band maxima are shifted (PC: 1588/1648 cm^{-1}, β-subunit: 1594/1654 cm^{-1}, see Figure 11). The fingerprint region is also quite different. In the β-subunit spectrum several bands are lacking: 1221 cm^{-1}, 1236 cm^{-1}, 1258 cm^{-1}. The 1246 cm^{-1} band, which is present in the β-subunit as well as in PC trimer spectra, does not vanish upon PCMS titration, as it does in PC trimer spectra. For β-subunits no PCMS effect could be detected in the CARS spectra. In principle, a PC trimer spectrum should be produced by the addition of a β-subunit spectrum (two chromophores: B84, B155) and an α-subunit spectrum (one chromophore: A84, whose structure in trimeric PC is similar to that of B84[38]). Though an α-subunit CARS spectrum is still lacking (in preparation), such an addition seems, however, to be impossible with the β-subunit spectrum shown in Figure 11a. Obviously, the distribution of chromophore structures is distinctly different in PC trimers and their investigated β-subunit preparation. The possible reasons are:

— variations in the interaction with the surrounding protein (eventually dependent on state of aggregation), while the gross geometry (extended, semi-extended or cyclic helical) is preserved.

— formation of different chromophore-protein arrangements during the process of preparation (denaturation-renaturation step).

— modified interaction with surrounding solvent in the subunits.

From the results of ps time-resolved measurements it has been concluded that in β-subunits the chromophores adopt a different gross geometry (semi-extended[52]).

The grade of structural identity of β-chromophores in PC and β-subunit preparations is of great importance, since in many studies results from β-subunit measurements are used to explain PC properties. The presented CARS spectra deny such a complete identity.

d) Allophycocyanin

The second kind of biliproteins from *Mastigocladus laminosus*, which we have investigated, are trimers, $(\alpha^{AP} \beta^{AP})_3$, without linker peptides of allophycocyanin (APC).

Like PC, APC is also constituted of α- and β-subunits with each subunit bearing only one phycocyanobilin chromophore (A84, B84).[34,36] In the visible spectral region APC monomers exhibit absorption similar to that of PC ($\lambda_{max} \approx 620$ nm).[54-57] In contrast, the absorption maximum of APC trimers appears at ≈ 650 nm.

Until now, there is only little knowledge about the structure of the chromophores. Despite the differences in amino acid sequences of both subunits[34] and the bathochromic shift of the absorption compared to PC, PC chromophore properties have been used to interpret life-time data of APC trimers[33,58]. Although we have begun our CARS investigations only recently, some remarkable conclusions can already be presented.

The comparison of CARS spectra demonstrates a distinct structural difference of the phycocyanobilin chromophores in PC and APC (Figure 10b, Figure 12). Highly interesting in this connection is also the difference of APC-CARS spectra recorded with different pump wavelengths (see Figure 12a, b, Table II). In the fingerprint region, the same vibrations appear, but with different intensities. The different relative intensities of the bands might be due to different resonance enhancement, which the two APC chromophores experience for 640 nm and 655 nm pump wavelengths, respectively. First of all, the weakness of the 1650 cm^{-1} vibration for 640 nm pump wavelength compared to its strength for $\lambda_p = 655$ nm is striking. This vibration is most probably indicative of an extended chromophore geometry, because it is present in resonance CARS and resonance Raman spectra[4] of PC trimers, while it is absent in vibrational spectra of non-extended tetrapyrrole chromophores. Therefore, it can be concluded that one chromophore adopts an extended geometry (strongly resonance enhanced at $\lambda_p = 655$ nm), whereas the other one, which dominates the resonance CARS spectrum at $\lambda_p = 640$ nm, adopts a non-extended geometry (see above).

Examples of non-extended chromophore geometry are biliverdin dimethyl-ester[48], denatured PC and free phycocyanobilin dissolved in chloroform[4] or the biliverdin IX$_\gamma$ biliprotein chromophore, isolated from the butterfly *Pieris brassicae* (Figure 8d).

e) The Pieris brassicae *Pigment*

Recent results of absorption, fluorescence and circular dichroism spectra[46] and a preliminary molecular model of the apoprotein deduced from X-ray data[47] claim that both apoprotein and chromophore of the *P. brassicae* pigment are very different from phycobiliproteins. The chromophore structure(s) should be similar to free biliverdin (cyclic helical geometry).

The absence of a band around 1650 cm^{-1} in the CARS spectrum of the *P. brassicae* pigment is another example (see Section g) that the presence / absence of this band is an indicator of extended / non-extended geometry of a tetrapyrrole chromophore.

From the above mentioned investigations[46,47], a relative high degree of conformational freedom of the biliverdin IX$_\gamma$ chromophore in the *P. brassicae* pigment is expected. On the other hand, the CARS spectrum displays a series of well-resolved bands with small linewidths all over the recorded range from 1100 cm^{-1} to 1650 cm^{-1}. This could be rationalized by the assumption that only those vibrations give rise to a strong CARS band which are rather localized and, therefore, less sensitive to small variations in structure. Such vibrations would be well-suited for the determination of chromophore gross structures (e. g. Z-E-isomerization), either by a comparison of vibrational spectra of different chromophores, or in connection with normal mode calculations.

CONCLUSION AND OUTLOOK

The given examples demonstrate that good quality CARS spectra can be reliably produced with the described experimental arrangement. The problem of dispersive line-shape can be overcome either by a suitable selection of the pump wavelength or by applying a least square line-fit procedure on the basis of equation 5. In some cases conclusions can be drawn even without a detailed analysis.

When studying biliproteins a number of advantages of CARS spectroscopy can be made use of. As even strong fluorescence does not perturb the recording of the vibrational spectra, the buffer solutions of the biliproteins can be studied at room temperature without application of specific sample preparation. Furthermore, the pump radiation can be chosen in resonance with the longest wavelength absorption band where changes in chromophore geometry exhibit the most pronounced effects. Therefore, even minor perturbations in chromophore structure, either due to modified chromophore protein interaction (e. g. effect of aggregation) or by forced perturbation (e. g. PCMS titration), can be detected rather easily.

By applying the transform theory[59,60], the values of the quotient R_r/I_r and the signs of R_r and I_r in dependence on the molecular frequency ν_r and the pump frequency ν_p can be derived from the absorption spectrum. Combination of such calculations with the line-fit procedure may improve the evaluation and interpretation of CARS spectra. Work in this direction is under way.[16]

With the progress in normal mode calculations and the availability of spectra of suitable model compounds, one should be able, in the near future, not only to detect differences in chromophore geometry, but also make state-

ments about the absolute geometry of the chromophore whose spectrum is recorded. The assignment of the various bands to specific molecular vibrations will be facilitated, when properly isotope-substituted samples are available (e. g. substitution of ^{14}N by ^{15}N). A knowledge of such isotope shifts would also provide a good test for our normal mode calculations using the method of Warshel[61,62] or that of Schachtschneider / Snyder[63].

So far, only phycocyanin from *Mastigocladus laminosus* and *Agmanellum quadruplicatum* could be crystallized and the X-ray analysis performed. Since only for these two biliproteins the coordinates of the chromophores are known within 2.1 Å resolution, most of the experimental and theoretical considerations have concentrated on them. In the discussion of spectroscopic results collected for biliproteins of other organisms, it is usually assumed that the arrangement of the chromophores is similar to that in *Mastigocladus laminosus*. The only technique, which seems presently to be able to prove such a hypothesis, is CARS spectroscopy. Our intention is, therefore, to apply this technique to biliproteins of different origins and in various states of aggregation. Furthermore, we will improve the normal mode calculations as an important means for the interpretation of the vibrational spectra.

REFERENCES

1. T. S c h i r m e r, W. B o d e, R. H u b e r, W. S i d l e r, and H. Z u b e r, *J. Mol. Biol.* **184** (1985) 257.
2. B. C u r r y, I. P a l i n g s, A. D. B r o e k, J. A. P a r d o e n, J. L u g t e n-b u r g, and R. M a t h i e s, in: *Advances in Infrared and Raman Spectroscopy*, Vol. 12, R. J. H. C l a r k and R. E. H e s t e r (Eds.), J. Wiley, Chichester 1985, p. 115—178.
3. B. S z a l o n t a i, Z. G o m b o s, and V. C s i z m a d i a, *Bochem. Biophys. Res. Commun.* **130** (1985) 358.
4. B. S z a l o n t a i, Z. G o m b o s, V. C s i z m a d i a, and M. L u t z, *Biochim. Biophys. Acta* **893** (1987) 296.
5. M. L u t z, in: *Advances in Infrared and Raman Spectroscopy*, Vol. 11, R. J. H. C l a r k and R. E. H e s t e r (Eds.), J. Wiley, Chichester 1984, p. 211—300.
6. P. D. M a k e r and R. W. T e r h u n e, *Phys. Rev.* **A137** (1965) 801.
7. F. W. S c h n e i d e r, in: *Non-Linear Raman Spectroscopy and Its Chemical Applications*, W. K i e f e r and D. A. L o n g (Eds.), D. Reidel Publishing Company, Dordrecht 1982, p. 445—460.
8. L. A. C a r r e i r a, L. P. G o s s, and T. B. M a l l o y Jr., in: *Chemical Applications of Nonlinear Raman Spectroscopy*, A. B. H a r v e y (Ed.), Academic Press, New York 1981, p. 321—376.
9. E. H o e x s t e r m a n n, W. W e r n c k e, I. N. S t a d n i c h u k, A. L a u, and P. H o f f m a n n, *Stud. Biophys.* **92** (1982) 147.
10. J. W. N i b l e r and G. V. K n i g h t e n, in: *Raman Spectroscopy of Gases and Liquids*, A. W e b e r (Ed.), Springer Verlag, Berlin, 1979, p. 253—300.
11. H. C. A n d e r s o n and B. S. H u d s o n, in: *Molecular Spectroscopy*, Vol. 5, *The Chemical Society*, London 1978, p. 142—201.
12. S. A. J. D r u e t, B. A t t a l, T. K. G u s t a f s o n, and J. P. T a r a n, *Phys. Rev.* **A18** (1978) 1529.
13. J. W. F l e m i n g and C. S. J o h n s o n Jr., *J. Raman Spec.* **8** (1979) 284.
14. U. K l ü t e r, *PhD Thesis*, Technical University, Munich (1986).
15. M. S. C a c e c i and W. P. C a c h e r i s, *Byte* **5** (1984) 340.
16. P. G e g e, *Diplomarbeit*, Technical University, Munich (1988).
17. J. T r e t z e l and F. W. S c h n e i d e r, *Chem. Phys. Lett.* **59** (1978) 514.

18. S. S c h n e i d e r, Z. *Phys. Chem. NF.* **154** (1987) 91.
19. *Photosynthetic Light-Harvesting Systems,* H. S c h e e r and S. S c h n e i d e r, (Eds.), Walter De Gruyter, Berlin 1988.
20. *Encyclopedia of Plant Physiology,* Vol. **19,** Photosyntehesis III, L. A. S t a e h e l i n and C. J. A r n t z e n (Eds.), Springer, Berlin 1988.
21. R. M a c C o l l and D. G u a r d - F r i a r, *Phycobiliproteins,* CRC Press, Boca Raton 1987.
22. H. S c h e e r, in: *Light Reaction Path of Photosynthesis,* F. K. F o n g (Ed.) Springer Verlag, Berlin 1982, 7—45.
23. E. G a n t t, C. A. L i p s c h u l t z, and F. X. C u n n i n g h a m Jr., in: Ref. 19, pp. 11—20.
24. E. G a n t, in: Ref. 20, 260—268.
25. E. M ö r s c h e l and E. R h i e l, in: *Electron Microscopy of Proteins,* Vol. **6,** *Membranous Structures,* J. R. H a r r i s and W. H o m e (Eds.), Academic Press, London 1987, pp. 209—254.
26. A. R. H o l z w a r t h, in: *The Light Reactions,* J. B a r b e r (Ed.), Elsevier, Amsterdam (1987), 95—157.
27. A. R. H o l z w a r t h, J. W e n d l e r, and G. S u t e r, *Biophys. J.* **51** (1987) 1.
28. S. S c h n e i d e r, P. G e i s e l h a r t, S. S i e b z e h n r ü b l, R. F i s c h e r, and H. S c h e e r, Z. *Naturforsch.* **43c** (1988) 55.
29. P. G e i s e l h a r t, *PhD Thesis,* Technical University, Munich (1988).
30. P. H e f f e r l e, W. J o h n, H. S c h e e r, and S. S c h n e i d e r, *Photochem. Photobiol.* **39** (1984) 221.
31. T. G i l l b r o, Å. S a n d s t r ö m, V. S u n d s t r ö m, R. F i s c h e r, and H. S c h e e r, in: Ref. 19, 457—468.
32. A. N. G l a z e r, S. W. Y e h, S. P. W e b b, and J. H. C l a r k, *Science* **227** (1985) 419.
33. P. M a x s o n, K. S a u e r, and A. N. G l a z e r, in: Ref. 19, 439—450.
34. H. Z u b e r, in: Ref. 20, 238—251.
35. G. F r a n k, W. S i d l e r, H. W i d m e r, and H. Z u b e r, *Hoppe-Seyler's Z. Physiol. Chem.* **359** (1978) 1491.
36. W. S i d l e r, J. G y s i, E. I s k e r, and H. Z u b e r, *Hoppe-Seyler's Z. Physiol. Chem.* **362** (1981) 611.
37. P. F ü g l i s t a l l e r, F. S u t e r, and H. Z u b e r, *Hoppe-Seyler's Z. Physiol. Chem.* **364** (1983) 691.
38. T. S c h i r m e r, W. B o d e, and R. H u b e r, *J. Mol. Biol.* **196** (1987) 677.
39. M. N i e s and W. W e h r m e y e r, *Planta* **150** (1980) 330.
40. W. K u f e r, O. S c h m i d, G. S c h m i d t, and H. S c h e e r, Z. *Naturforsch.* **41c** (1986) 437.
41. P. F ü g l i s t a l l e r, H. W i d m e r, W. S i d l e r, G. F r a n k, and H. Z u b e r, *Arch. Microbiol.* **129** (1981) 268.
42. S. S i e b z e h n r ü b l, R. F i s c h e r, and H. S c h e e r, Z. *Naturforsch.* **42c** (1987) 258.
43. S. S c h n e i d e r, F. B a u m a n n, and U. K l ü t e r, Z. *Naturforsch.* **42c** (1987) 1269.
44. R. F i s c h e r, private communication.
45. H. K a y s e r, in: *Comprehensive Insect Physiology, Biochemistry and Pharmacology,* G. A. K e r k u t and L. I. G i l b e r t, eds., Pergamon Press, New York (1985) 367—415.
46. H. S c h e e r and H. K a y s e r, Z. *Naturforsch.* **43c** (1988) 84.
47. R. H u b e r, M. S c h n e i d e r, O. E p p, I. M a y r, A. M e s s e r s c h m i d t, J. P f l u g r a t h, and H. K a y s e r, *J. Mol. Biol.* **195** (1987) 423.
48. L. M a r g u l i e s and M. T o p o r o w i c z, *J. Am. Chem. Soc.* **106** (1984) 7331.
49. S. S c h n e i d e r, P. G e i s e l h a r t, F. B a u m a n n, H. F a l k, and W. M e d i n g e r, *J. Photochem, Photobiol., B: Biology* **2** (1988) 233.
50. S. S c h n e i d e r, C. S c h a r n a g l, and W. S t e i n e r, manuscript in preparation.
51. M. D u e r r i n g, private communication.
52. S. S c h n e i d e r, P. G e i s e l h a r t, F. B a u m a n n, S. S i e b z e h n r ü b l, R. F i s c h e r, and H. S c h e e r, in: Ref. 19, 469—482.

53. S. Schneider, F. Baumann, P. Geiselhart, S. Siebzehnrübl, R. Fischer, and H. Scheer, in: *Proceedings of the Second European Conference on the Spectroscopy of Biological Molecules*, J. Wiley, Chichester (1988).
54. R. MacColl, K. Csatorday, D. S. Berns, and E. Traeger, *Biochemistry* **19** (1980) 2817.
55. M. Mimuro, A. Murakami, and Y. Fujita, *Arch. Biochem. Biophys.* **215** (1982) 266.
56. A. Murakami and Y. Fujita, *Photochem. Photobiol.* **38** (1983) 605.
57. S. W. Yeh, A. N. Glazer, and J. H. Clark, *J. Phys. Chem.* **90** (1986) 4578.
58. E. Bittersmann, W. Reuter, W. Wehrmeyer, and A. R. Holzwarth, in Ref. 19, 451—456.
59. P. M. Champion and A. C. Albrecht, *Chem. Phys. Lett.* **82** (1981) 410.
60. M. Pfeiffer, A. Lau, and W. Wernecke, *J. Raman Spec.* **15** (1984) 20.
61. A. Warshel and M. Karplus, *J. Am. Chem. Soc.* **94** (1972) 5612.
62. A. Warshel and M. Levitt, *QCPE Program* No. 247. Revised Version 1973.
63. J. H. Schachtschneider, *Shell Technical Report* No. 57—65 (1965), Modification by G. Baranović.
64. S. Siebzehnrübl, private communication.

SAŽETAK

Rezonantno pojačana CARS spektroskopija biliproteina

Siegfried Schneider, Franz Baumann, Ulrich Klüter i Peter Gege

Dan je pregled teorijskih i eksperimentalnih aspekata uključenih u CARS spektroskopiju višeatomnih molekula u otopinama. Prikazani su rezonantno pojačani CARS spektri različitih biliproteina (APC**, PC** i njegovih podjedinica) iz cijanobakterija *mastigocladus laminosus* u različitim stanjima agregacije, te raspravljeni s obzirom na informacije koje se mogu izvesti o strukturi tetrapirolnih kromofora. Zaključuje se, da se zbog agregacije mijenjaju kromoforna svojstva uslijed interakcije kromofor-protein bilo promjenom konformacije konfiguracije, bilo promjenom proteinske okoline kromofora (mikroheterogenost). Suprotno široko prihvaćenoj pretpostavci, geometrija kromofora mora biti različita za APC i PC.